Annals of Biomedical Engineering, Vol. 30, pp. 483–497, 2002
Printed in the USA.

0090-6964/2002/30(4)/483/15/$15.00

Image-Based Computational Fluid Dynamics Modeling in Realistic Arterial Geometries

DAVID A. STEINMAN

Imaging Research Laboratories, The John P. Robarts Research Institute, and Departments of Medical Biophysics and Diagnostic Radiology and Nuclear Medicine, The University of Western Ontario, London, Ontario, Canada

(Received 23 July 2001; accepted 3 December 2001)

Abstract—Local hemodynamics are an important factor in atherosclerosis, from the development of early lesions, to the assessment of stroke risk, to determining the ultimate fate of a mature plaque. Until recently, our understanding of arterial fluid dynamics and their relationship to atherosclerosis was limited by the use of idealized or averaged artery models. Recent advances in medical imaging, computerized image processing, and computational fluid dynamics (CFD) now make it possible to computationally reconstruct the time-varying, three-dimensional blood flow patterns in anatomically realistic models. In this paper we review progress, made largely within the last five years, towards the routine use of anatomically realistic CFD models, derived from *in vivo* medical imaging, to elucidate the role of local hemodynamics in the development and progression of atherosclerosis in large arteries. In addition to describing various image-based CFD studies carried out to date, we review the medical imaging and image processing techniques available to acquire the necessary geometric and functional boundary conditions. Issues related to accuracy, precision, and modeling assumptions are also discussed. © *2002 Biomedical Engineering Society.* [DOI: 10.1114/1.1467679]

Keywords—Computational fluid dynamics, Hemodynamics, Medical imaging, 3D reconstruction, Finite-element method.

INTRODUCTION

Atherosclerosis is the leading cause of mortality and morbidity in the western world. The observation that atherosclerotic plaques typically occur at arterial bifurcations and bends has led to the now almost universal acceptance that local hemodynamic factors, in particular, wall shear stresses (WSS), play a role in the disease's initiation and, perhaps more importantly, its progression.[50] Despite the fact that three decades have passed since the original hemodynamic hypotheses of atherosclerosis were first postulated,[7,21] much remains unclear regarding the relative importance and relevance of the many proposed hemodynamic factors.[3,8,21,32,41,44] This is due in part to the fact that studies correlating local hemodynamic factors with lesion distributions have been, until recently, *retrospective*,[19,20,41] necessarily relying on idealized or averaged hemodynamic models and postmortem measurements of vessel wall pathology. Required now are *prospective* studies in which local hemodynamic and disease indices are measured and directly correlated in a subject-specific and, ideally, noninvasive manner.

In principle, magnetic resonance and ultrasound imaging can be used to measure both wall thickness (a marker for atherosclerotic burden) and blood velocities (from which WSS can be derived) directly in human subjects. In practice, however, such an ''imaging only'' approach has been successfully applied only to relatively straight vessels,[24,25,38,39,60] owing to the implicit assumption of uniform flow that underlies most *in vivo* velocimetry techniques. It is in regions of complex flow, however, such as at the carotid bifurcation, where atherosclerotic plaques typically develop.

In the last 15 years, computational fluid dynamics (CFD) has proven to be a practical and reliable tool for studying time-varying, three-dimensional (3D) blood flow patterns in complex, albeit idealized, arterial geometries. Briefly, in CFD modeling, a complex geometry is discretized into a large number of smaller but regular (typically, tetrahedral or hexahedral) *elements*. By assuming the shape of the velocity field within these elements, it is possible to solve the governing Navier–Stokes equations at the *nodes* connecting these elements. From this solution it is straightforward to extract WSS and other important hemodynamic quantities. Moreover, in contrast to experimental flow studies, it is trivial to alter model parameters such as flow rates, wall properties, etc. This has made CFD a particularly attractive tool for hemodynamics research. Nevertheless, as noted by Meairs *et al.*,[51] ''*[n]umerical simulation of blood flow could be particularly useful in the elucidation of complex interactions between pulsatile flow, plaque and vessel geometry, and wall elasticity. The study of such phenomena, however, will necessarily require that numerical simulation*

Address correspondence to David A. Steinman, PhD, Imaging Research Laboratories, The John P. Robarts Research Institute, 100 Perth Drive, London, Ontario N6A 5K8 , Canada. Electronic mail: steinman@irus.rri.ca

move beyond its experimental model phase and begin incorporating actual clinical data as parameter inputs for simulation.'' With the convergence of high-resolution medical imaging, sophisticated image processing techniques and high-performance desktop workstations in the last five years, such image-based CFD studies of *in vivo* hemodynamics are now possible.

In this paper we review the medical imaging and reconstruction methods used to provide the boundary conditions for the CFD simulation. Selected *in vivo* applications of medical image-based CFD techniques to elucidate the role of local hemodynamics in atherosclerosis of the large arteries are described. Finally, important issues related to the assessment of accuracy and precision, and the impact of the assumptions on which these model studies are based, are discussed.

METHODS

X-ray Imaging

The first image-based CFD studies of anatomically realistic arterial geometries were derived from clinical x-ray angiograms.[22,73] In its modern form, x-ray angiography involves the acquisition of projection images following the intra-arterial injection of an iodinated contrast agent, which causes the vessel lumen to be highlighted. For cardiac applications, images are typically acquired at high frame rates in order to capture the vessel motion and contrast agent dynamics. For less dynamic vessels such as the carotid artery, single or multiplane projections are more typically acquired, from which corresponding preinjection images are digitally subtracted to remove background bone and tissue, further highlighting the vessel lumen. Figure 1 shows such a digital subtraction angiogram (DSA), which in this case was used to reconstruct a *two-dimensional* (2D) model of a carotid bifurcation.[73] Reconstruction of *three-dimensional* models requires at least two (ideally orthogonal) projections, and some assumptions about the shape of the lumen cross sections. Alternatively, recent advances in x-ray imaging technology make possible the rapid (4–6 s) acquisition of multiple (~200) projection images,[15] from which the 3D lumen geometry can be reconstructed at high (200–400 μm isotropic) spatial resolution without the need for *a priori* assumptions about lumen shape.

The advantage of x-ray angiography over other medical imaging modalities is the superior (and, to date, unsurpassed) contrast-to-noise ratio, combined with high temporal and spatial resolution. The price paid for this quality is the finite risk associated with catheterization, which is in fact greater than the risk associated with the radiation dose itself.[5] (A less invasive alternative is to inject contrast intravenously, and rapidly acquire the 3D volume using single or multiple ring helical CT scanners; however, this approach typically produces poorer contrast images of the lumen.) As a result, it is difficult to carry out human studies of early atherosclerosis and local hemodynamics using x-ray angiography, since it is typically performed only for patients with known or suspected vascular disease. Furthermore, DSA alone cannot provide information about the state of the vessel wall, making it impossible to determine the true plaque burden. Finally, although in principle x-ray imaging can also be used to measure blood flow rates *in vivo*,[68] these techniques remain largely experimental, and thus not yet practical for image-based CFD studies.

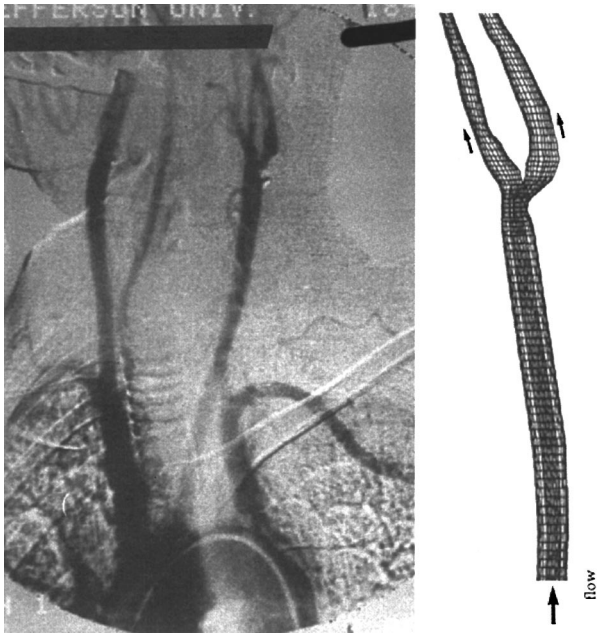

FIGURE 1. (Left) A digital subtraction angiogram used to construct (right) a two-dimensional model of the carotid bifurcation. From Tasciyan *et al.* (Ref. 73), with permission.

In spite of these limitations, x-ray imaging is likely to continue to play an important role in image-based CFD studies. No other imaging modalities can yet provide the dynamic information needed to track intravascular probes (e.g., intravascular ultrasound; see below) or construct realistic models of *in vivo* coronary artery dynamics. And, unlike optical sectioning techniques, micro-CT scanners can readily provide high (100–200 μm isotropic) resolution images of vascular casts or specimens in a nondestructive manner.[53,57]

Magnetic Resonance Imaging

Unlike x-ray imaging, magnetic resonance imaging (MRI) does not require the use of ionizing radiation. Instead, contrast is achieved by exploiting differences in the magnetic spin relaxation properties of the various bodily tissues and fluids. For the purposes of imaging blood vessels, MRI is particularly attractive since the blood itself can be used as a contrast agent. Signal from

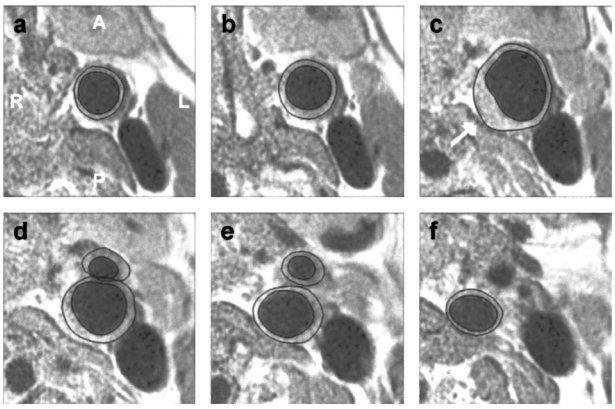

FIGURE 2. Cropped black blood MR images showing semi-automatically segmented inner and outer boundary contours, from selected locations along the carotid bifurcation. Such contours from the full series of ~30 images were used to reconstruct the lumen and wall geometries for the model shown in Fig. 9. From Steinman *et al.* (Ref. 72), with permission.

flowing blood can, for example, be enhanced at the expense of signal from static surrounding tissue, producing images analogous to x-ray angiograms. Such ''bright blood'' MR angiograms do, however, tend to suffer from relatively poor signal quality (or lower spatial resolution) as compared to their x-ray counterparts, and regions of slowly flowing or recirculating blood, such as the carotid bulb, can induce signal loss. This had led to use of intravenous paramagnetic agents (e.g., gadolinium DTPA) that alter the relaxation characteristics of blood, providing a more flow independent method of contrast. Such *contrast-enhanced* MR angiography (ceMRA) is becoming a viable alternative to x-ray angiography for noncardiac vessels, and recent work suggests that isotropic resolutions of 600 μm may soon be achievable in scan times of 1–2 min.[67] The negligible risk associated with the use of MR contrast agents makes it easier to justify their use in asymptomatic patients and normal volunteers, which helps explain the popularity of ceMRA as a source of high-quality geometric data for image-based CFD studies of large artery hemodynamics.[46,47,49,74,81,85,87]

An alternative to conventional angiography, which provides information only about the lumen boundary, is ''black blood'' MRI—so named because the signal from flowing blood is suppressed rather than enhanced. As demonstrated in Fig. 2, this allows both the inner and outer boundaries of the vessel wall to be imaged at relatively high resolutions (~300 μm in plane, 1.5–2 mm slice thickness), from which both lumen geometry and vessel wall thickness can be determined in a noninvasive manner. We have recently demonstrated the use of such black blood MRI for reconstructing maps of wall thickness and shear stresses in a subject-specific manner,[72] highlighting the potentially broad applicability of these techniques for longitudinal studies of atherosclerosis development in humans. Black blood MRI is, of course, not without its limitations, the most notable being the potential for plaque mimicking slow flow artifacts, which can be minimized, but not always eliminated, through judicious selection of imaging parameters.[70] Due to the presence of periadventitial tissue, we have also found that it is often difficult to achieve adequate contrast at the outer boundary of the vessel wall, which degrades the reliability of wall thickness measurements.[43] Although not yet exploited in the context of image-based CFD studies, recent work suggests that wall boundaries can be enhanced through the use of MR contrast agents, whose dynamics may also provide important information about vascular wall pathology.[1]

In addition to its abilities to define the vessel lumen and wall, MRI is perhaps the most powerful technique available for imaging blood velocities *in vivo*. Phase contrast MRI (PC-MRI)—so named because the velocity is encoded into the phase of the complex MRI signal—can be used to provide 2D or, less commonly, 3D *images* of one or more velocity components in a time-resolved, but not real-time, manner. We have demonstrated that PC-MRI can accurately measure time-varying velocities under uniform flow conditions;[18] however, in the presence of complex flow patterns, such as at the carotid bifurcation, velocity images (and hence velocity accuracy) can be distorted by a number of artifacts.[69] As a result, PC-MRI is most commonly used in image-based CFD applications for providing flow rate wave forms at the relatively straight inlet and outlet segments of complex vessel geometries. Flow rates are obtained by integrating the velocities over the user- or computer-identified lumen, and used to impose fully developed (i.e., Womersley) velocity boundary conditions at the model inlets and, optionally, outlets.[52] The PC-MRI velocities themselves may be applied directly to the CFD model by interpolating the image grid onto the inlet nodes,[46] but this requires more sophisticated postprocessing techniques and higher-quality PC-MRI images at the further expense of scan time.

For the purposes of CFD modeling in distensible vessels, PC-MRI may also be used to estimate the subject-specific pressure wave form and elastic modulus. As recently noted by Cebral and co-workers,[11,12] instantaneous flow rates measured along the length of the carotid bifurcation by PC-MRI may not necessarily be the same, owing to the attenuation and shift of the pressure and flow rate wave forms induced by the compliance of the vessel. This observation led them to estimate the pressure drop between the inlet and outlet of the model using a one-dimensional (1D) lumped parameter model and an assumed value for the elastic modulus. By fixing the inlet flow rate and inlet/outlet pressure drop wave form

in a subsequent 3D CFD simulation, they were able to ''tune'' the elasticity modulus to produce the best match between the computed and measured outlet flow rates.

Ultrasound Imaging

Of all vascular imaging technologies, ultrasound is perhaps the most widely available, owing to the relatively low cost of ultrasound scanners. An ultrasound image is formed by transmitting a high-frequency (1–10 MHz) beam into the body, and collecting and analyzing the returned echoes to produce an image whose intensity is related to the echogenicity of the tissue and tissue interfaces. Because image quality in ultrasound is determined largely by the proximity of the transducer to the tissue of interest, ultrasound imaging is typically limited to superficial vessels such as the carotid and femoral arteries.

Ultrasound imaging of vascular anatomy, though commonly used in the clinic, has yet to play a significant role in image-based CFD analysis. This is because the 2D ultrasound images, unlike MRI or x-ray images, are acquired manually without reference to a fixed coordinate system, making it difficult to reconstruct a series of them in 3D. By sweeping an electronically tracked ultrasound transducer along the length of the vessel either manually or mechanically, however, one can construct 3D ultrasound images with high ($0.2\times0.2\times0.6\,\mathrm{mm}^3$) effective spatial resolution in less than 10 s.[16] Although we have shown that it is possible to reconstruct lumen geometry directly from such 3D ultrasound data,[23] the overall image quality does not yet appear sufficient—especially in comparison to MRI—for the purposes of reliable CFD calculations. With new ''compound'' ultrasound imaging techniques,[35] however, we have begun to see improvements in the quality of 3D ultrasound images that may eventually render them useful for image-based CFD analysis.

In contrast to conventional *extravascular* ultrasound, *intravascular* ultrasound (IVUS) has played a significant role in several image-based CFD modeling studies.[13,34,40,45,83] As illustrated in Fig. 3, a high-resolution IVUS transducer is introduced via catheter into the artery where, owing to its proximity, it can acquire detailed images of the vessel wall structure. X-ray angiography is used to guide the placement of the transducer, and also to orient the (2D) ultrasound imaging planes for the 3D reconstruction of the inner and outer boundaries of the vessel. As these are highly invasive procedures, IVUS-based CFD modeling studies have been limited to animal models, or to patients already referred for cardiac catheterization. Although this naturally precludes the study of early atherosclerosis in otherwise healthy subjects, IVUS will continue to play an important role in the *in vivo* study of the otherwise inaccessible coronary arteries. Furthermore, IVUS remains the most sensitive of all imaging techniques for the purposes of simultaneously reconstructing local hemodynamics and vascular wall pathology *in vivo*.

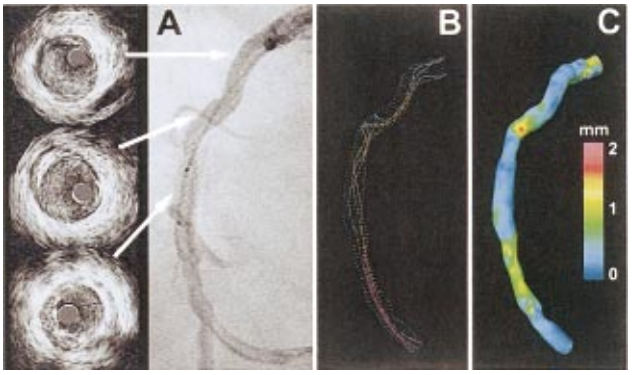

FIGURE 3. (A) IVUS images acquired along the segment of right coronary artery shown (with catheter) in an angiographic view, from which (B) local hemodynamics and (C) wall thickness were reconstructed. From van Langenhove *et al.* (Ref. 78), with permission.

As with MRI, ultrasound may also be used to measure blood velocities *in vivo*. Unlike PC-MRI, which provides spatially resolved velocity maps at the expense of temporal resolution, Doppler ultrasound is typically used to provide real-time measurements of the velocities at the nominal centerline of the vessel, from which the mean velocity and, given the vessel radius, flow rate, can be calculated assuming a fully developed velocity profile.[29] Alternatively, the velocities at a series of points along a vessel radius can be measured, from which a more refined estimate of the flow rate can be obtained by assuming axisymmetry of the velocity profile.[45] Either way, however, these assumptions limit the application of Doppler ultrasound in image-based CFD analysis to estimating flow in relatively straight inlet sections where uniform flow patterns can reasonably be expected.

Ultrasound may also be used to estimate the regional mechanical properties of the vessel wall, as demonstrated by Vonesh *et al.*[79] In this case IVUS was used to reconstruct a 3D model of a tissue specimen, which was subjected to finite-element structural analysis. By loading both the model and real specimen with the same pressures, the regional tissue properties could be tuned to minimize differences between the computed and IVUS-measured wall displacements.

Finally, as demonstrated by Zhao and co-workers[85,87] in CFD studies of realistically distensible carotid bifurcation models, a number of different ultrasound techniques can be used together to provide the necessarily boundary conditions in a noninvasive and subject-specific manner. In this case inlet and outlet flow rate wave forms were measured using Doppler ultrasound. The inlet pressure wave form was measured by placing a

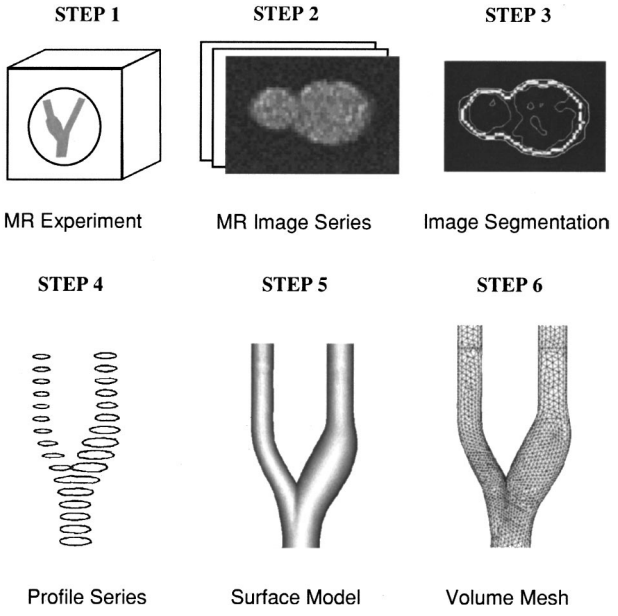

FIGURE 4. Summary of typical steps required for the construction of a finite-element mesh from serial images. From Moore *et al.* (Ref. 55).

high-fidelity external pressure transducer above the pulsating carotid artery. Intima–media thickness measured from B-mode images was used to estimate the wall thickness at two locations along the common carotid artery, and one location in each of the branches. To determine wall mechanical properties, an approach similar to that of Vonesh *et al.*[79] was employed. The measured diameter and wall thickness were used to construct a tubular model of the common carotid artery, which was loaded with the measured pressure wave form, and then deformed using finite-element structural analysis. The wall elasticity was then tuned to match the computed displacements against previously acquired M-mode ultrasound measurements of the carotid artery wall displacements.

Reconstruction of 3D Vessel Geometry

The typical steps involved in the construction of a 3D CFD model from serial medical images are shown in Fig. 4. Given a series of 2D cross-sectional images of the vessel, the most obvious method of reconstruction is to outline, either manually or with computer assistance, the boundaries of the lumen—and, if available, the outer wall—to produce a skeleton of the vessel. Many techniques are then available for converting this series of profiles into a 3D surface model. For straight or curved vessels without branches, such as coronary artery segments, it is straightforward to connect corresponding points around the circumference of the vessel, using splines or filtering techniques to achieve a desired level of smoothing.[40] For bifurcating or branching vessels one may use the above-described approach to reconstruct each branch separately, and then merge them using solid modeling operations.[17]

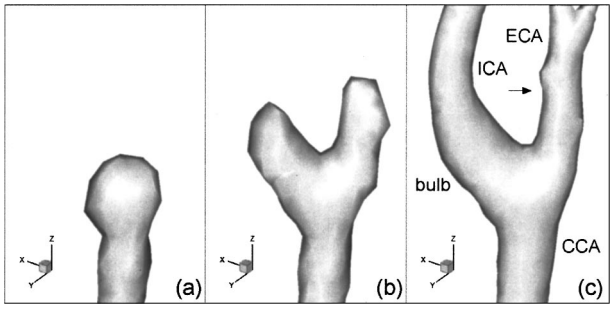

FIGURE 5. Stages in the 3D discrete dynamic contour segmentation of a carotid bifurcation from black blood MR images. Note the ability to naturally seep into vessel branches. From Ladak *et al.* (Ref. 42), with permission.

With the increasing availability of high-resolution, 3D image data of complex, branching vascular structures, it becomes impractical to outline what may amount to hundreds of individual vessel contours. Instead, more sophisticated image processing techniques must be employed. One approach, presented by Wang *et al.*,[81] is to extract from the 3D image volume individual 2D images distributed along and oriented normal to the centerlines of vessels of interest (as identified by an operator). These 2D images may then be processed as described above for conventional serial images.

An alternative approach is to operate on the 3D image volume directly, by extending 2D contour detection algorithms to 3D. Towards this end we have developed a 3D discrete dynamic contour (DDC) for identifying the vessel lumen from a stack of serial black blood MR images[42] and 3D ultrasound volumes.[23] Analogous to inflating a balloon inside the 3D images, an operator merely places within the lumen a triangulated sphere, which is then driven towards the lumen boundaries, where it is refined via the same internal and image-based forces used for the 2D DDC upon which it was based.[43] Figure 5 illustrates the key advantage of this novel approach; namely, its ability to ''seep'' into branches without operator intervention. This is not without its disadvantages, most notably the difficulty in avoiding side branches that may not be of interest. In the absence of robust 3D editing tools, a reasonable compromise is offered by Yim *et al.*,[84] who used 3D tubular deformable models to produce a smoothed, triangulated surface for each vessel branch of interest. These discrete, triangulated surfaces were then merged in a manner analogous to the Boolean merging of continuous, solid models.[10]

Volume Mesh Generation

The final but key step in the vessel reconstruction process is the discretization of the complex model into finite elements or volumes, whose size and distribution largely govern the accuracy of the computed velocity field: smaller elements must be used to resolve the more complex flow regions, but the computational requirements scale with the number of elements used. Thus, a nontrivial balance must be struck between solution accuracy and computational effort.

For simple geometries that are topologically equivalent to a straight tube, such as coronary artery segments, meshing is fairly straightforward and can be easily automated by dividing the tube-like structure into a fixed number of points around the circumference and along the tube axis.[40] Such *structured* meshes may also be generated for bifurcating geometries, though considerably more effort is required to ensure the quality of the elements.[48] More popular are *unstructured* meshes in which arbitrary distributions of tetrahedral, hexahedral, or prismatic elements are generating using a variety of sophisticated algorithms.[77] The advantage of this approach is that meshes can be readily generated for arbitrarily complex geometries using widely available mesh generation tools. Still, these approaches typically rely on the user to identify regions where increased mesh density may be required to adequately resolve the velocity field.

An alternative approach is to use *adaptive refinement*, in which the computed velocity field itself is used to guide the placement of the finite elements. As presented by Prakash and Ethier[65] for a realistic coronary artery model, the velocity field is first computed using a relatively coarse, uniform mesh. The local solution error is then estimated and used to guide the automatic subdivision of elements only where the predicted error is greatest.[64] Iteration of this procedure results in a volume mesh that is highly resolved only where it is needed, thus maximizing the solution accuracy while minimizing the computational effort. To date, however, adaptive refinement techniques have only been developed for use with steady flows, though such adapted meshes may of course be used subsequently for pulsatile flow simulations.

APPLICATIONS

One of the first applications of image-based CFD was to study the relationship between WSS and atherosclerosis progression.[22] In this case a group of patients was followed for three years via cine angiography of their coronary arteries. The vessel centerlines and boundaries were identified from the angiographic projection images in a semiautomated manner and, assuming circular cross sections, used to reconstruct 2D axisymmetric CFD models of the coronary segments. The same steady flow rate was assumed for all vessels. For each of the 20 segments studied, the change in vessel diameter over time was compared against the corresponding WSS computed in the base-line geometry, at an average of 70 locations along the length of the vessel. A statistically significant inverse relationship between these variables was observed in 15 of the 20 segments, providing some of the first direct *in vivo* evidence that low WSS promotes the progression of atherosclerotic lesions.

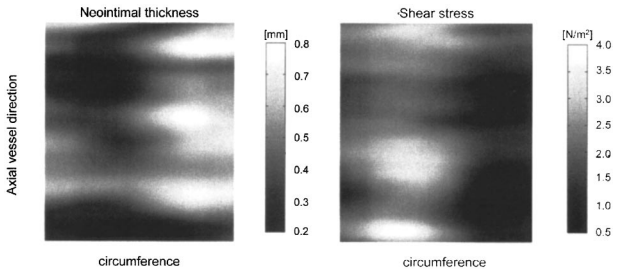

FIGURE 6. Maps of neointimal thickness (left) and wall shear stress (right) from a stented human coronary artery segment demonstrate a clear inverse relationship. From Wentzel *et al.* (Ref. 83), with permission.

Several years later, Krams *et al.*[40] applied the angiography and ultrasound (ANGUS) approach to quantify wall thickness and WSS in a 3D model of a human coronary segment derived from a clinical angiographic image taken at end diastole. Uniform steady inflow velocities were assumed. A representative circumferential distribution of wall thickness and WSS values was obtained by averaging the respective values along the vessel length. Maximal and minimal WSS were found to occur on the outer and inner walls, respectively, as expected. When compared to the circumferential distribution of wall thickness, a statistically significant inverse relationship was found, consistent with the low shear hypothesis of atherosclerosis.

A number of applied studies using this ANGUS approach have since been carried out to elucidate the role of WSS in cardiac interventional procedures. In a follow-up study of a patient who had undergone coronary stenting, van Langenhove *et al.*[78] observed helical flow and low WSS at a site upstream of the stent where local wall thickening was also observed (see Fig. 3). Conversely, the presence of only mild neointimal hyperplasia at the stented site was attributed to the relatively undisturbed flow and higher WSS seen at this location. The relationship between stent restenosis and WSS was further examined by Wentzel *et al.*[83] in a study of 14 patients. WSS was computed in 3D (steady flow) models reconstructed from the IVUS images, while the thickness of the neointima in the stented region was inferred by measuring the distance between the lumen surface and stent contours from the IVUS images. As Fig. 6 illus-

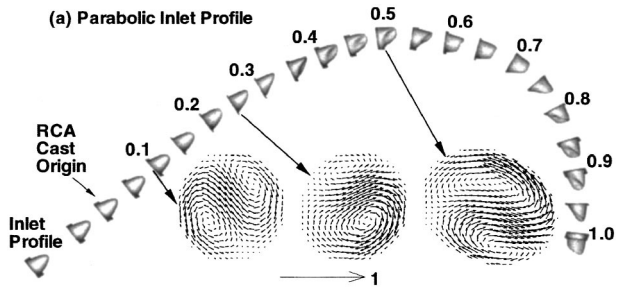

FIGURE 7. Steady flow velocity profiles and secondary flow patterns demonstrating the complex rotation of the velocity field induced by secondary geometric effects. From Myers *et al.* (Ref. 57).

trates, a significant inverse relationship between WSS and neointimal thickness was observed, suggesting the important role that local hemodynamics may play in the success or failure of interventional procedures. Most recently, Wentzel *et al.*[82] demonstrated how image-based CFD techniques may be used to elucidate the mechanisms by which both fluid and wall stresses participate in the vascular remodeling process. In this case 12 pigs were imaged using ANGUS both before and six weeks after percutaneous transluminal angioplasty (PTA) of the external iliac artery. Half of the pigs were given Batimastat [a matrix metalloproteinase (MMP) inhibitor previously demonstrated to help modulate vascular remodeling] while the other half served as a control group. For the control group both WSS and wall stress (as inferred from Laplace's formula) normalized to their respective values at a reference segment of the vessel after six weeks, while in the Batimastat group only the WSS normalized. This study concluded that vascular remodeling after PTA is controlled by both WSS and wall stress, but that MMP inhibition inhibits the wall stress control system.

To date most IVUS-based CFD studies of coronary artery hemodynamics have assumed steady flow, with the implicit assumption that these models provide a faithful representation of the time-averaged hemodynamics. A more detailed image-based CFD study of pulsatile coronary artery hemodynamics was recently carried out by Myers *et al.*[57] in a model of the human right coronary artery reconstructed from high-resolution CT images of a flow-through acrylic model previously constructed from a cast of a specimen. The key finding of this study (as illustrated in Fig. 7) was that relatively small amounts of out-of-plane curvature had a dramatic effect on the skewing of the axial velocity profiles and orientation of the secondary flow vortices along the length of the vessel. This was manifested as a marked variability in the orientation of low and high WSS regions away from their nominal locations along the inner and outer curves of the vessel. Interestingly, the time-averaged WSS behavior from both sinusoidal and physiologically pulsatile flow studies was similar to that from a corresponding steady flow study, supporting the use of steady flow models for the purposes of inferring time-averaged behavior. This study and others[34,36] highlight the sensitivity of coronary artery blood flow patterns to local geometric features, and also underline the importance of subject-specific geometry when trying to draw conclusions about the localization of atherosclerotic lesions from individual vessels.

In the area of atherosclerosis research, the carotid bifurcation is perhaps the most widely studied blood vessel. Aside from its obvious clinical importance in relation to stroke, the relatively large size and superficial location of the carotid arteries provide an ideal window for external ultrasound transducers and MRI surface coils, whose proximity to the vessel of interest largely determines the quality of the resulting images. This noninvasive window makes the carotid bifurcation an ideal target for image-based CFD techniques since, unlike the coronary artery, it allows for the study of normal volunteers or asymptomatic patients, and thus atherosclerosis even at its early stages.

We presented one of the first studies of normal subject-specific carotid bifurcation hemodynamics,[52] using black blood and cine phase contrast MRI to reconstruct 3D lumen geometries and time-varying inlet and outlet flow. Maps of a variety of WSS indices showed obvious qualitative differences in patterns between the two subjects studied; however, as Fig. 8 demonstrates, more pronounced differences were observed between the *in vivo* models and an idealized normal carotid bifurcation model. Secondary helical flow patterns were found to play a key role in determining the resulting WSS patterns, while the use of the subject-specific flow rate wave form was found to have a minor but noticeable effect on the WSS patterns. This study clearly demonstrated how averaged or idealized carotid bifurcation models can mask interesting hemodynamic features that may be of importance in understanding the localization of individual lesions.

Refinement of our black blood imaging and image analysis techniques[42,43,76] has since made it possible to simultaneously reconstruct 3D maps of both WSS *and* wall thickness in a subject-specific manner. Application of this approach to a patient with early atherosclerosis and a normal volunteer showed a qualitative association between increased wall thickness at the carotid bulb and low and oscillating shear (Fig. 9).[72] When pooling data from all points on the surface, however, no statistically significant relationship between mean or oscillating shear and wall thickness could be found. Although it is possible that no such simple relationship exists, it is also possible that the inability to resolve intimal thickness itself, or other possible sources of inaccuracy or imprecision, may have masked such a relationship. Neverthe-

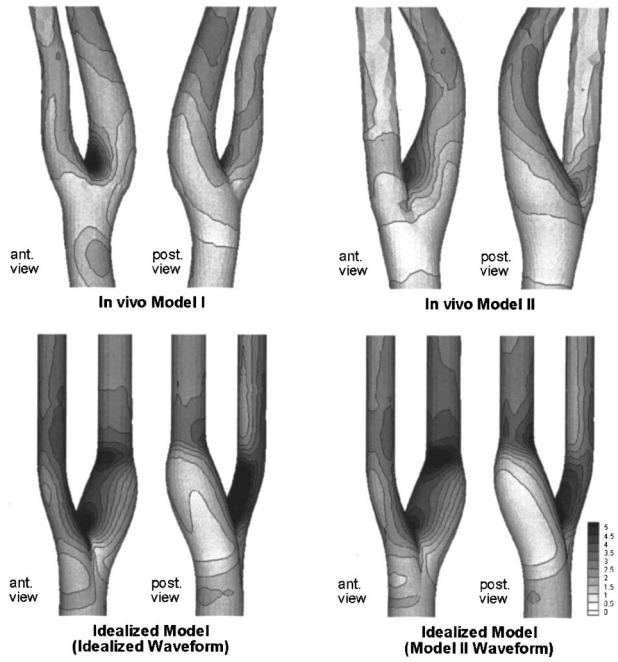

FIGURE 8. Magnitude of time-averaged normalized wall shear stress in normal human and idealized carotid bifurcation models. Note the subject-specific nature of the wall shear stress patterns, as well as the marked differences as compared to the idealized model. From Milner *et al.* (Ref. 52), with permission.

less, this black blood MRI-based approach is currently the sole alternative for studying the relationship between local hemodynamics and vascular disease in a prospective and noninvasive manner.

In the interest of simplicity, to date our CFD analyses have been confined to rigid walled vessels, based on the assumption that wall distensibility has only a minor effect on the *distribution* of WSS (see the Discussion). Recent work by Zhao *et al.*[87] has demonstrated the feasibility of carrying out detailed fluid-structure interaction modeling studies of realistic carotid bifurcation. As described above in the Methods, a novel feature of this work is the use of various ultrasound imaging techniques to provide branch flow rates, local wall thickness, and wall elastic modulus in a subject-specific manner. (The nominal lumen geometry must still be derived using contrast-enhanced MRA; however, this group is currently investigating the use of 3D ultrasound to provide the lumen geometry.[2]) Application of these techniques to five normal subjects showed significant intersubject variations in the magnitude and distribution of WSS and mechanical stress.[85] More significant was the finding that regions of low WSS and high mechanical stresses tended to overlap at sites where plaques are known to typically occur (Fig. 10), providing preliminary, albeit circumstantial, evidence for the combined role that forces at *and* within the wall may play a role in atherogenesis.

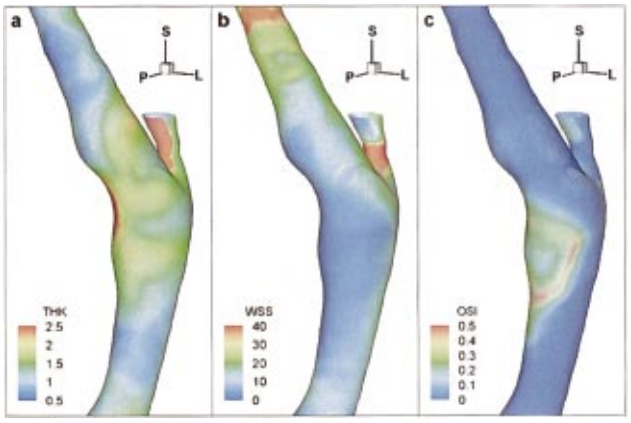

FIGURE 9. Increased wall thickness (left) at the carotid bulb of a patient with early atherosclerosis is shown to be associated with low mean (middle) and high oscillating (right) wall shear stress. From Steinman *et al.* (Ref. 72), with permission.

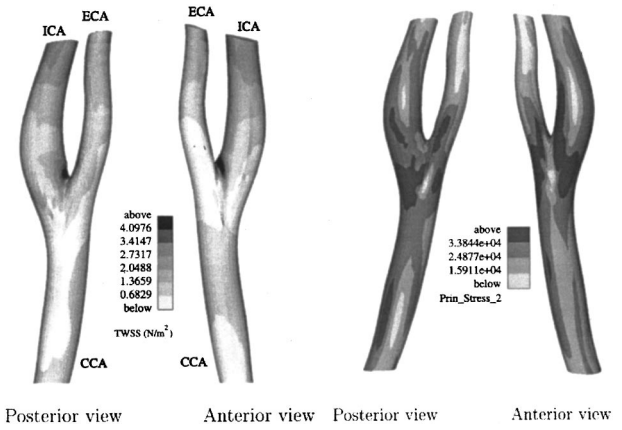

FIGURE 10. Maps of (left) time-averaged wall shear stress and (right) principal wall stresses from a coupled fluid-structure interaction model of a human carotid bifurcation. From Zhao *et al.* (Ref. 87), with permission.

Further evidence for the interaction between fluid and wall mechanical forces was provided by Liu *et al.*,[45] who carried out pulsatile flow simulations in models of carotid and femoral artery segments reconstructed from IVUS imaging of Yucatan miniswine. Rather than attempt to model the wall motion directly, in which case, as shown above, the individual wall properties should be measured, IVUS was used to acquire the vessel geometry at different times during the cardiac cycle. The resulting 3D reconstructions were then used to drive a moving-boundary CFD simulation of the pulsatile hemodynamics. The time-varying inlet velocity profiles were prescribed based on Doppler ultrasound measurements from four locations along a vessel diameter. The key finding from this study was that the phase angle between the

computed WSS and the measured hoop strain (i.e., diameter change) was strongly affected by local changes in geometry, providing further direct evidence that a complex coupling of fluid and mechanical forces may be important in the development of atherosclerosis.

DISCUSSION

Accuracy

A number of studies have attempted to demonstrate the accuracy of computed hemodynamics in anatomically realistic arteries. Perktold *et al.*[62] constructed physical and numerical models from the same cast of a human left coronary artery branch. Physiologically pulsatile axial velocities were measured at selected locations using laser-Doppler anemometry. The same flow conditions were imposed on the 3D CFD model, and generally good agreement between the corresponding velocity profiles was observed. In a similar study, Botnar *et al.*[6] constructed physical and experimental models of a human carotid artery bifurcation specimen. In this case, time-resolved 2D PC-MRI was used to measure both axial and secondary velocities. Very good qualitative agreement was observed between the experimental and numerical velocities, with quantitative differences of less than 10% for axial peak flow velocities. Some disagreement was seen in the size and shape of the secondary vortices, but circumferential velocities were within the same overall range. More recently, Myers *et al.*[57] observed good qualitative agreement between WSS computed in a model of a right coronary artery, and WSS measured in a matching acrylic cast using photochromic dye tracer techniques.

These studies provide compelling evidence that CFD can reliably model flow in complex, realistic artery geometries. Alone, however, they are not sufficient for determining whether a reconstructed model is faithfully reproducing the *in vivo* hemodynamic environment. Such *direct* validation of computationally reconstructed local hemodynamics is difficult in the absence of a gold-standard technique for measuring velocities *in vivo* (which, if it existed, would of course obviate the need for computational reconstructions). PC-MRI offers the greatest promise as an *in vivo* gold standard, but still suffers from a number of artifacts that become more apparent in the context of physiologically pulsatile and complex flow. Nevertheless, we[72] and others[46,47] have reported generally good qualitative agreement between computed and PC-MRI imaged *in vivo* velocity patterns, providing comforting but inconclusive evidence that image-based CFD models are physiologically faithful. As the accuracy of PC-MRI is practically—but not fundamentally—limited, further improvements in MRI hardware and software may eventually render PC-MRI a viable gold standard for *in vivo* velocimetry.

In the similar absence of a gold standard for high-resolution imaging of lumen geometry *in vivo*, it is also difficult to assess the accuracy of the reconstructed geometries. Moore *et al.*[53] compared lumen geometries reconstructed from *in vivo* ceMRA imaging of six rabbit aortoiliac bifurcations against those reconstructed from CT imaging of casts or specimens of the same vessels. The process of pressure fixing or casting was found to induce alterations in vessel paths and bifurcation angles, but ceMRA-based models tended to underpredict aortic dimensions immediately proximal to the bifurcation. These geometric differences led to marked differences in computed WSS and flow separation patterns at the hips of the bifurcation, amounting to 15%–35% differences in mean WSS. In a related study, Moore *et al.*[55] reconstructed models of a mathematically defined, idealized normal carotid bifurcation from MR imaging of an acrylic flow-through model of the known geometry filled with static fluid. Geometric errors were found to be less than 150 μm, within the specified precision of the acrylic model itself. WSS values computed in the reconstructed models agreed to within less than 15%, providing a lower bound for the accuracy with which WSS can be reconstructed from image-based CFD models.

Another potential source of error in image-based CFD has little to do with the quality of the images or reconstructions themselves: the resolution of the finite-element mesh. Normally, a mesh is considered sufficiently resolved when a doubling of the element size (or, more commonly but less satisfactorily, the number of elements) induces little change in the computed velocity field. As Prakash and Ethier[65] recently demonstrated through the use of adaptively refined meshes, extremely fine local mesh densities are required to resolve WSS (i.e., the *gradient* of the velocity field) to within 10%. Although this suggests that virtually all image-based CFD studies to date are under-resolved in terms of element density, the authors did note that WSS *patterns* were reliably predicted even at the lower mesh resolutions.

In summary, it is important to retain some perspective regarding the significance of absolute errors in WSS, whatever the source, given the many assumptions and trade offs involved in image-based CFD analysis (see below). As proposed by Moore *et al.*,[53] errors in WSS should be considered significant only if they would ''lead to different conclusions regarding the likely cause or location of vascular disease.'' Given the inability to resolve these models down to the level of endothelial cell morphology, it is reasonable to consider current image-based CFD models wholly satisfactory if they can predict WSS *patterns*, rather than absolute WSS *values*, faithfully.

Reproducbility and Precision

Many questions can be asked whose answers determine the precision with which image-based CFD models can be reconstructed from a set of medical images. How noisy are the source images? How reliably can an operator extract the wall boundaries? How reliably can a 3D model be reconstructed from the extracted wall boundaries? Does repeated imaging of the same subject lead to the same results? Answers to these questions determine whether local differences in computed WSS patterns, or changes over time as detected by longitudinal studies of hemodynamics and vascular disease, are real or mere artifacts of the reconstruction process. In the context of our black blood MRI-based CFD techniques, we are now attempting to answer some of these important questions.

To determine the precision with which a given operator can extract the inner and outer wall boundaries from black blood MRI images, four operators were asked to segment 12 different images three times each, using both manual and computer-assisted techniques. After dividing each boundary into eight equal sectors, the precision with which local radius and wall thickness were reproduced by the operators was determined using analysis of variance (ANOVA) techniques. As detailed in Ladak *et al.*,[43] we found that lumen boundary and wall thickness could be reproduced to within approximately 100 μm, and that interoperator variability was only slightly higher than intraoperator variability. From this same analysis, it was also possible to estimate the minimum changes in these variables that could be significantly detected in a longitudinal study. We later used the results of this study to show that the semiautomated segmentation allowed us to degrade the subjective image quality (by increasing spatial resolution at the expense of reduced signal-to-noise ratios) without substantially affecting precision.[76]

More recently, we have begun to address the issue of intrasubject variability by repeatedly imaging the same patients at weekly intervals, in which case any differences in reconstructed hemodynamics and wall thickness may be attributed to reconstruction variability. Preliminary (unpublished) results from this work suggest that the 3D lumen geometry may be reproduced to within less than 300 μm, while time-averaged WSS values are precise to within less than 4 dyn/cm^2. Moreover, mean and oscillatory WSS *patterns* appear to be consistent among the repeated reconstructions. This provides the most direct evidence to date for the sensitivity with which we will be able to detect changes in geometric and hemodynamic variables in longitudinal studies.

The precision of the reconstructed model is also strongly influenced by the level of smoothing used. Too much smoothing may mask genuine arterial morphology, while too little smoothing can preserve spurious, small-scale variations in the lumen geometry induced by the imaging, segmentation, and/or reconstruction. The need for some smoothing was demonstrated by Moore *et al.*[54] using a straight tube model reconstructed from MR angiography. Without smoothing, spurious errors in WSS were 30%–40% of the nominal value; with smoothing, these errors were reduced to less than 10%. In a subsequent study of a bypass graft specimen imaged using high-resolution CT,[56] the removal of small-scale geometric features was found not to significantly change the flow and WSS distributions. As demonstrated by Long *et al.*,[48] smoothing is also important for models reconstructed from serial 2D imaging, owing to the real possibility of subject and, in the absence of gating, vessel motion between slice acquisitions.

Finally, an important source of variability rarely considered is that associated with normal physiological fluctuations, which can range from normal cycle-to-cycle variations in heart and flow rates, to acute changes in cardiac output (e.g., rest versus exercise) and posture (e.g., sitting versus supine). It is of interest to note that, for practical reasons related to scanner geometry, the majority of images used for image-based CFD studies are acquired with the subject resting in a supine position. The flexibility and temporal resolution of Doppler ultrasound provides perhaps the best means of acquiring data for CFD studies of these various physiological states, in order to help establish the normal variability of the CFD boundary conditions and, more importantly, their effect on the variability of the computed local hemodynamics. Open bore MRI scanners can also provide such information, but they continue to be relatively scarce.

Modeling Assumptions

Viscosity. In a study of flow in a realistic carotid bifurcation model, Perktold and Hofer[61] reported slightly higher WSS values using a non-Newtonian versus Newtonian viscosity model. However, overall WSS patterns were preserved, which is largely consistent with previous reports in idealized models.

Distensibility. In their recent study of a distensible human carotid bifurcation model, Zhao *et al.*[87] observed a general reduction in the magnitude of WSS, but the global characteristics of the flow and stress patterns remained unchanged. This was attributed to the fact that the global pressure derives the wall motion, while flow-related local pressure gradients had only a minor influence. These findings are consistent with results from a CFD study of pulsatile flow in compliant and rigid models of a carotid bifurcation cast.[37] As suggested by Cebral,[11] however, distensibility may have a more subtle effect on image-based CFD modeling of healthy arteries. By inducing measurable changes in the dynamics of the

flow rate wave forms over the length of the vessel, wall distensibility can produce apparent mismatches in the inlet and outlet flow rate boundary conditions that can only be reconciled with a distensible CFD model. For imaging older subjects or patients with vascular disease, however, this effect is likely minimal owing to increased vessel stiffness. On a related note, most large arteries are tethered to surrounding tissue, in which case the effect of bulk motion is likely to be even less than that associated with distensibility. For coronary arteries, however, the situation is almost certainly reversed. Given the demonstrated sensitivity of WSS distributions to local curvature in coronary artery models, it is very possible that fixed, rigid models of the coronary arteries do not reproduce the true intracoronary blood flow patterns. It remains to be seen, however, whether these effects are ''hemodynamically significant.''

Side Branches. In most image-based CFD studies, small side branches arising from the vessel(s) of interest are ignored, largely because they are often difficult to resolve using *in vivo* imaging techniques, especially if they are oriented parallel to the (often thick) imaging slice planes. A number of recent studies have, however, shown that these small branches have only a relatively minor effect on the local hemodynamics elsewhere.[14,58,86] As image-based CFD models become more sophisticated, and begin to include such branches, it will not be practical to individually measure the flow rates (and pressures) at each branch for the purposes of establishing physiological boundary conditions. Instead, techniques for computing the boundary conditions based on models of the vascular resistance will become increasingly important.[59]

Flow Conditions. Although it is obvious that steady flow CFD models are not capable of reproducing the complex, *time-varying* behavior of physiological flow patterns, recent studies[45,57] have shown that they do provide a reasonable approximation to the *time-averaged* WSS behavior. Furthermore, both studies demonstrated that the shape of the inlet velocity profile (i.e., uniform versus fully developed versus realistic) has little effect on downstream flow patterns beyond a relatively short entrance length. Both studies concluded that geometrical factors drive the flow, further evidence that efforts to improve the quality of image-based CFD should focus primarily on geometric fidelity. Having said this, it is important to remember that the effects of inlet velocity profile and flow wave-form shape are strongly influenced by the Reynolds and Womersley numbers associated with the vessel of interest. For example, we[52] noted secondary but non-negligible effects on mean WSS patterns at a carotid bifurcation after altering the shape of the physiological flow wave form. This may be a reflection of the fact that Womersley numbers at the carotid bifurcation ($\sim$5) are higher than those in the coronary artery segments ($\sim$2) where flow effects were found to be negligible.

Practical Limitations

The most obvious practical limitation associated with image-based CFD analysis is the significant amount of computational effort required to execute a single model. When Taylor *et al.*[75] published one of the first image-based CFD studies, of an abdominal aorta model composed of $\sim$300,000 linear tetrahedral finite elements, they reported an execution time of 10 h per cardiac cycle on an eight-processor SGI workstation. More recently, Cebral (personal communication) has reported execution times of approximately 4 h per cardiac cycle on a four-processor SGI workstation for a $\sim$1,000,000 element model. Our own studies are currently carried out on relatively inexpensive, single processor 1 GHz Pentium III workstations, with execution times for equivalently resolved models of 16–24 CPU hours per cardiac cycle. Given the seeming inevitability of Moore's law alone, we may anticipate an order of magnitude increase in execution time over the next five years. Coupled to CFD software and operating systems that can readily take advantage of multiple processors, it is likely that well-resolved CFD studies will be executed on small clusters of cheap desktop workstations in minutes rather than hours.

Although computational effort may ultimately determine the time between acquisition and results, the real effort involved in image-based CFD modeling occurs well before the CFD simulation is initiated. Converting image data into the necessary CFD boundary conditions typically requires specialized software, experienced operators, and hours of manpower. A number of operator-dependent decisions must typically be made during the reconstruction process, which increases the likelihood of bias and imprecision. It is, however, difficult to fully automate this process, given the different imaging modalities, varying vessel geometries, and especially the varying quality of source images. Instead, robust and user-friendly techniques that can help an operator turn a set of medical images into a CFD input file in a matter of minutes are required. Tools developed by Taylor and co-workers[74,81] for the purposes of computer-assisted planning of vascular surgery offer a glimpse into the future of routine image-based CFD analysis.

Future Directions

In the past five years, image-based CFD modeling has moved from the qualitative to the quantitative, and is now beginning to gain acceptance for the purposes of basic and applied vascular research. With the growing

body of knowledge related to the cellular, molecular, and genetic responses to hemodynamic factors, we can envision a closer coupling between image-based CFD and biological models for the purposes of predicting—rather than merely confirming—the development, progression, and, perhaps, even therapeutically induced regression of atherosclerosis in individual vessels.

As high-resolution medical imaging and image processing techniques become more robust, we can also anticipate clinical applications of image-based modeling. This is perhaps most straightforwardly illustrated by the ''predictive medicine'' techniques being developed by Taylor *et al.*[74] to assist vascular surgeons in planning and predicting, in a patient-specific manner, the outcome of different treatment strategies. Similarly, Guadagni *et al.*[28] and Cebral *et al.*[9] have proposed the use of MRI-based CFD models for evaluating different strategies for the surgical repair of, respectively, congenital heart defects and cerebral aneurysms. We have also begun developing x-ray angiography-based CFD techniques for the purposes of understanding, optimizing, and, eventually, planning minimally invasive, neuroradiologically guided therapies for intracranial aneurysms. Anatomically realistic models, for now derived from *ex vivo* data, have also been used to evaluate the specific surgical techniques employed for carotid endarterectomy[31,33] and peripheral bypass grafting.[63]

As proposed by Raghavan *et al.*,[66] x-ray CT-based finite-element models of abdominal aortic aneurysms may be used to better predict rupture of individual aneurysms and thus improve the management of patients with this disease. Similarly, image-based modeling may be useful for identifying classes of advanced atherosclerotic lesions—and, eventually, individual patients—that are vulnerable to rupture and/or thrombotic events. Early steps in this direction have already been taken by using *ex vivo* imaging of plaque specimens to provide realistic models for 2D image-based CFD[4] and finite-element[30] analyses. We[71,80] have also demonstrated how a patient-specific CFD model could be used to help resolve conflicting diagnostic information arising from a follow-up duplex ultrasound examination of a postendarterectomy patient.

Finally, it should be noted that, owing to the practical difficulty associated with resolving the microvasculature and modeling the complex rheology at that level, medical image-based CFD modeling studies will likely always be limited to large arteries. As demonstrated by Goldman and Popel,[26,27] however, anatomically realistic models of the microcirculation, perhaps derived from *ex vivo* or even *in vivo* microscopy, may be useful for predicting oxygen transport under normal and pathological conditions.

ACKNOWLEDGMENTS

The author acknowledges the support of a Heart & Stroke Foundation of Ontario Grant-in-aid (T-3739), and a Heart & Stroke Foundation of Canada Research Scholarship.

REFERENCES

[1] Aoki, S., K. Aoki, S. Ohsawa, H. Nakajima, H. Kumagai, and T. Araki. Dynamic MR imaging of the carotid wall. *J. Magn. Reson. Imaging* 9:420–427, 1999.

[2] Augst, A. D., D. C. Barratt, A. D. Hughes, S. A. Thom, and X. Y. Xu. CFD model of a human carotid artery bifurcation reconstructed from 3D ultrasound data. Proceedings of the 5th International Symposium on Computer Methods in Biomechanics and Biomedical Engineering, 2001 (unpublished).

[3] Bao, X., C. Lu, and J. A. Frangos. Temporal gradient in shear but not steady shear stress induces PDGF-A and MCP-1 expression in endothelial cells: Role of NO, NF kappa B, and egr-1. *Arterioscler., Thromb., Vasc. Biol.* 19:996–1003, 1999.

[4] Stroud, J. S., S. A. Berger, and D. Saloner. Numerical analysis of flow through a severely stenotic carotid artery bifurcation. *J. Biomech. Eng.* 124:9–20, 2002.

[5] Bergeron, P., R. Carrier, D. Roy, N. Blais, and J. Raymond. Radiation doses to patients in neurointerventional procedures. *AJNR Am. J. Neuroradiol.* 15:1809–1812, 1994.

[6] Botnar, R., G. Rappitsch, M. B. Scheidegger, D. Liepsch, K. Perktold, and P. Boesiger. Hemodynamics in the carotid artery bifurcation: A comparison between numerical simulations and *in vitro* MRI measurements. *J. Biomech.* 33:137–144, 2000.

[7] Caro, C. G., J. M. Fitz-Gerald, and R. C. Schroter. Atherosclerosis and arterial wall shear: Observations, correlation, and proposal of a shear-dependent mass transfer mechanism for atherogenesis. *Proc. R. Soc. London, Ser. B* 177:109, 1971.

[8] Caro, C. G., J. M. Fitz-Gerald, and R. C. Schroter. Proposal of a shear-dependent mass transfer mechanism for atherogenesis. *Clin. Sci.* 40:5P, 1971.

[9] Cebral, J. R., R. Lohner, and J. E. Burgess. Computer simulation of cerebral artery clipping: Relevance to aneurysm neurosurgery planning. Proceedings of the European Congress on Computational Methods in Applied Sciences and Engineering, 2000 (unpublished).

[10] Cebral, J. R., R. Lohner, P. L. Choyke, and P. J. Yim. Merging of intersecting triangulations for finite-element modeling. *J. Biomech.* 34:815–819, 2001.

[11] Cebral, J. R., R. Lohner, O. Soto, and P. J. Yim. On the modeling of carotid artery blood flow from magnetic resonance images. *ASME Bioeng. Conf.* 50:619–620, 2001.

[12] Cebral, J. R., P. J. Yim, R. Lohner, O. Soto, H. Marcos, and P. J. Choyke. New methods for computational fluid dynamics modeling of carotid artery from magnetic resonance angiography. *Proc. SPIE* 4321:177–187, 2001.

[13] Chandran, K. B., M. J. Vonesh, A. Roy, S. Greenfield, B. Kane, R. Greene, and D. D. McPherson. Computation of vascular flow dynamics from intravascular ultrasound images. *Med. Eng. Phys.* 18:295–304, 1996.

[14] Clingan, P. A., and M. H. Friedman. The effect of celiac and renal artery outflows on near-wall velocities in the porcine iliac arteries. *Ann. Biomed. Eng.* 28:302–308, 2000.

[15] Fahrig, R., A. J. Fox, S. Lownie, and D. W. Holdsworth. Use

of a C-arm system to generate true three-dimensional computed rotational angiograms: Preliminary *in vitro* and *in vivo* results. *AJNR Am. J. Neuroradiol.* 18:1507–1514, 1997.
[16] Fenster, A., D. B. Downey, and H. N. Cardinal. Three-dimensional ultrasound imaging. *Phys. Med. Biol.* 46:R67–R99, 2001.
[17] Foutrakis, G. N., G. Burgreen, H. Yonas, and R. J. Sclabassi. Construction of 3D arterial volume meshes from magnetic resonance angiography. *Neurol. Res.* 18:354–360, 1996.
[18] Frayne, R., D. A. Steinman, C. R. Ethier, and B. K. Rutt. Accuracy of MR phase contrast velocity measurements for unsteady flow. *J. Magn. Reson. Imaging* 5:428–431, 1995.
[19] Friedman, M. H., C. B. Bargeron, O. J. Deters, G. M. Hutchins, and F. F. Mark. Correlation between wall shear and intimal thickness at a coronary artery branch. *Atherosclerosis (Berlin)* 68:27–33, 1987.
[20] Friedman, M. H., O. J. Deters, C. B. Bargeron, G. M. Hutchins, and F. F. Mark. Shear-dependent thickening of the human arterial intima. *Atherosclerosis (Berlin)* 60:161–171, 1986.
[21] Fry, D. L. Acute vascular endothelial changes associated with increased blood velocity gradients. *Circ. Res.* 22:165–197, 1968.
[22] Gibson, C. M., L. Diaz, K. Kandarpa, F. M. Sacks, R. C. Pasternak, T. Sandor, C. Feldman, and P. H. Stone. Relation of vessel wall shear stress to atherosclerosis progression in human coronary arteries. *Arterioscler. Thromb.* 13:310–315, 1993.
[23] Gill, J. D., H. M. Ladak, D. A. Steinman, and A. Fenster. Accuracy and variability assessment of a semiautomatic technique for segmentation of the carotid arteries from three-dimensional ultrasound images. *Med. Phys.* 27:1333–1342, 2000.
[24] Gnasso, A., C. Carallo, C. Irace, V. Spagnuolo, N. G. De, P. L. Mattioli, and A. Pujia. Association between intima-media thickness and wall shear stress in common carotid arteries in healthy male subjects. *Circulation* 94:3257–3262, 1996.
[25] Gnasso, A., C. Irace, C. Carallo, F. M. De, C. Motti, P. L. Mattioli, and A. Pujia. *In vivo* association between low wall shear stress and plaque in subjects with asymmetrical carotid atherosclerosis. *Stroke* 28:993–998, 1997.
[26] Goldman, D., and A. S. Popel. Computational modeling of oxygen transport from complex capillary networks. Relation to the microcirculation physiome. *Adv. Exp. Med. Biol.* 471:555–563, 1999.
[27] Goldman, D., and A. S. Popel. A computational study of the effect of capillary network anastomoses and tortuosity on oxygen transport. *J. Theor. Biol.* 206:181–194, 2000.
[28] Guadagni, G., F. Migliavacca, G. Dubini, and E. L. Bove. Simulations of surgical planning for fontan procedures. *Proc. ASME Bioeng. Conf.* 50:911–912, 2001.
[29] Holdsworth, D. W., C. J. Norley, R. Frayne, D. A. Steinman, and B. K. Rutt. Characterization of common carotid artery blood-flow wave forms in normal human subjects. *Physiol. Meas.* 20:219–240, 1999.
[30] Huang, H., R. Virmani, H. Younis, A. P. Burke, R. D. Kamm, and R. T. Lee. The impact of calcification on the biomechanical stability of atherosclerotic plaques. *Circulation* 103:1051–1056, 2001.
[31] Hyun, S., C. Kleinstreuer, and J. P. Archie, Jr. Computer simulation and geometric design of endarterectomized carotid artery bifurcations. *Crit. Rev. Biomed. Eng.* 28:53–59, 2000.
[32] Hyun, S., C. Kleinstreuer, and J. P. Archie, Jr. Hemodynamics analyses of arterial expansions with implications to thrombosis and restenosis. *Med. Eng. Phys.* 22:13–27, 2000.
[33] Hyun, S., C. Kleinstreuer, and J. P. Archie, Jr. Computational particle-hemodynamics analysis and geometric reconstruction after carotid endarterectomy. *Comput. Biol. Med.* 31:365–384, 2001.
[34] Ilegbusi, O. J., Z. Hu, R. Nesto, S. Waxman, D. Cyganski, J. Kilian, P. H. Stone, and C. L. Feldman. Determination of blood flow and endothelial shear stress in human coronary artery *in vivo*. *J. Invasive Cardiol.* 11:667–674, 1999.
[35] Jespersen, S. K., J. E. Wilhjelm, and H. Sillesen. Multiangle compound imaging. *Ultrason. Imaging* 20:81–102, 1998.
[36] Kaazempur-Mofrad, M. R., and C. R. Ethier. Mass transport in an anatomically realistic human right coronary artery. *Ann. Biomed. Eng.* 29:121–127, 2001.
[37] Karner, G., K. Perktold, M. Hofer, and D. Liepsch. Flow characteristics in an anatomically realistic compliant carotid artery bifurcation model. *Comput. Methods Biomech. Biomed. Eng.* 2:171–185, 1999.
[38] Kornet, L., A. P. Hoeks, J. Lambregts, and R. S. Reneman. In the femoral artery bifurcation, differences in mean wall shear stress within subjects are associated with different intima–media thicknesses. *Arterioscler., Thromb., Vasc. Biol.* 19:2933–2939, 1999.
[39] Kornet, L., J. Lambregts, A. P. Hoeks, and R. S. Reneman. Differences in near-wall shear rate in the carotid artery within subjects are associated with different intima–media thicknesses. *Arterioscler., Thromb., Vasc. Biol.* 18:1877–1884, 1998.
[40] Krams, R., J. J. Wentzel, J. A. Oomen, R. Vinke, J. C. Schuurbiers, P. J. de Feyter, P. W. Serruys, and C. J. Slager. Evaluation of endothelial shear stress and 3D geometry as factors determining the development of atherosclerosis and remodeling in human coronary arteries *in vivo*. Combining 3D reconstruction from angiography and IVUS (ANGUS) with computational fluid dynamics. *Arterioscler., Thromb., Vasc. Biol.* 17:2061–2065, 1997.
[41] Ku, D. N., D. P. Giddens, C. K. Zarins, and S. Glagov. Pulsatile flow and atherosclerosis in the human carotid bifurcation. Positive correlation between plaque location and low oscillating shear stress. *Arteriosclerosis (Dallas)* 5:293–302, 1985.
[42] Ladak, H. M., J. S. Milner, and D. A. Steinman. Rapid three-dimensional segmentation of the carotid bifurcation from serial MR images. *J. Biomech. Eng.* 122:96–99, 2000.
[43] Ladak, H. M., J. B. Thomas, J. R. Mitchell, B. K. Rutt, and D. A. Steinman. A semiautomatic technique for measurement of arterial wall from black blood MRI. *Med. Phys.* 28:1098–1107, 2001.
[44] Lei, M., C. Kleinstreuer, and G. A. Truskey. A focal stress gradient-dependent mass transfer mechanism for atherogenesis in branching arteries. *Med. Eng. Phys.* 18:326–332, 1996.
[45] Liu, Y., Y. Lai, A. Nagaraj, B. Kane, A. Hamilton, R. Greene, D. D. McPherson, and K. B. Chandran. Pulsatile flow simulation in arterial vascular segments using intravascular ultrasound images. *Med. Eng. Phys.* 23:583–595, 2001.
[46] Long, Q., X. Y. Xu, B. Ariff, S. A. Thom, A. D. Hughes, and A. V. Stanton. Reconstruction of blood flow patterns in a human carotid bifurcation: A combined CFD and MRI study. *J. Magn. Reson. Imaging* 11:299–311, 2000.
[47] Long, Q., X. Y. Xu, M. Bourne, and T. M. Griffith. Numerical study of blood flow in an anatomically realistic aorto-iliac bifurcation generated from MRI data. *Magn. Reson. Med.* 43:565–576, 2000.
[48] Long, Q., X. Y. Xu, M. W. Collins, M. Bourne, and T. M. Griffith. Magnetic resonance image processing and structured grid generation of a human abdominal bifurcation. *Comput. Methods Programs Biomed.* 56:249–259, 1998.
[49] Long, Q., X. Y. Xu, M. W. Collins, T. M. Griffith, and M.

Bourne. The combination of magnetic resonance angiography and computational fluid dynamics: A critical review. *Crit. Rev. Biomed. Eng.* 26:227–274, 1998.
[50] Malek, A. M., S. L. Alper, and S. Izumo. Hemodynamic shear stress and its role in atherosclerosis. *J. Am. Med. Assoc.* 282:2035–2042, 1999.
[51] Meairs, S., J. Rother, W. Neff, and M. Hennerici. New and future developments in cerebrovascular ultrasound, magnetic resonance angiography, and related techniques. *J. Clin. Ultrasound* 23:139–149, 1995.
[52] Milner, J. S., J. A. Moore, B. K. Rutt, and D. A. Steinman. Hemodynamics of human carotid artery bifurcations: Computational studies with models reconstructed from magnetic resonance imaging of normal subjects. *J. Vasc. Surg.* 28:143–156, 1998.
[53] Moore, J. A., B. K. Rutt, S. J. Karlik, K. Yin, and C. R. Ethier. Computational blood flow modeling based on *in vivo* measurements. *Ann. Biomed. Eng.* 27:627–640, 1999.
[54] Moore, J. A., D. A. Steinman, and C. R. Ethier. Computational blood flow modeling: Errors associated with reconstructing finite-element models from magnetic resonance images. *J. Biomech.* 31:179–184, 1998.
[55] Moore, J. A., D. A. Steinman, D. W. Holdsworth, and C. R. Ethier. Accuracy of computational hemodynamics in complex arterial geometries reconstructed from magnetic resonance imaging. *Ann. Biomed. Eng.* 27:32–41, 1999.
[56] Moore, J. A., D. A. Steinman, S. Prakash, K. W. Johnston, and C. R. Ethier. A numerical study of blood flow patterns in anatomically realistic and simplified end-to-side anastomoses. *J. Biomech. Eng.* 121:265–272, 1999.
[57] Myers, J. G., J. A. Moore, M. Ojha, K. W. Johnston, and C. R. Ethier. Factors influencing blood flow patterns in the human right coronary artery. *Ann. Biomed. Eng.* 29:109–120, 2001.
[58] Myers, J. G., M. Ojha, K. W. Johnston, and C. R. Ethier. Influence of branches, curvature, and caliber on blood flow patterns in the human right coronary artery. *Comput. Methods Biomech. Biomed. Eng.* (in press).
[59] Olufsen, M. S. Structured tree outflow condition for blood flow in larger systemic arteries. *Am. J. Physiol.* 276:H257–H268, 1999.
[60] Pedersen, E. M., S. Oyre, M. Agerbaek, I. B. Kristensen, S. Ringgaard, P. Boesiger, and W. P. Paaske. Distribution of early atherosclerotic lesions in the human abdominal aorta correlates with wall shear stresses measured *in vivo*. *Eur. J. Vasc. Endovasc. Surg.* 18:328–333, 1999.
[61] Perktold, K., and M. Hofer. Mathematical modeling of flow effects and transport processes in arterial bifurcation models. In The Haemodynamics of Arterial Organs—Comparison of Computational Predictions with *In vivo* and *In vitro* Data, edited by X. Y. Xu and M. W. Collins. Southampton, UK: WIT, 1999, pp. 43–84.
[62] Perktold, K., M. Hofer, G. Rappitsch, M. Loew, B. D. Kuban, and M. H. Friedman. Validated computation of physiologic flow in a realistic coronary artery branch. *J. Biomech.* 31:217–228, 1998.
[63] Perktold, K., A. Leuprecht, M. Prosi, T. Berk, M. Czerny, W. Trubel, and H. Schima. Fluid dynamics, wall mechanics, and oxygen transfer in peripheral bypass anastomoses: Computer studies on various designs. *Ann. Biomed. Eng*. (in press).
[64] Prakash, S., and C. R. Ethier. Enhanced error estimator for adaptive finite-element analysis of 3D incompressible flow. *Comput. Methods Appl. Mech. Eng*. 190:5413–5426, 2001.
[65] Prakash, S., and C. R. Ethier. Requirements for mesh resolution in 3D computational hemodynamics. *J. Biomech. Eng.* 123:134–144, 2001.
[66] Raghavan, M. L., D. A. Vorp, M. P. Federle, M. S. Makaroun, and M. W. Webster. Wall stress distribution on three-dimensionally reconstructed models of human abdominal aortic aneurysm. *J. Vasc. Surg.* 31:760–769, 2000.
[67] Rutt, B. K., D. W. Holdsworth, S. Naik, D. H. Lee, and A. J. Fox. Ultra-high-resolution three-dimensional carotid MRA: Validation of ceMRA and MOTSA with CRA. Proceedings of the International Society for Magnetic Resonance in Medicine 9th Scientific Meeting, 2001, p. 399.
[68] Shpilfoygel, S. D., R. A. Close, D. J. Valentino, and G. R. Duckwiler. X-ray videodensitometric methods for blood flow and velocity measurement: A critical review of literature. *Med. Phys.* 27:2008–2023, 2000.
[69] Steinman, D. A., C. R. Ethier, and B. K. Rutt. Combined analysis of spatial and velocity displacement artifacts in phase contrast measurements of complex flows. *J. Magn. Reson. Imaging* 7:339–346, 1997.
[70] Steinman, D. A., and B. K. Rutt. On the nature and reduction of plaque-mimicking flow artifacts in black blood MRI of the carotid bifurcation. *Magn. Reson. Med.* 39:635–641, 1998.
[71] Steinman, D. A., J. B. Thomas, H. M. Ladak, J. S. Milner, J. G. Merino, and J. D. Spence. Use of a patient-specific computational hemodynamic model to explain conflicting Doppler and B-mode ultrasound assessments of carotid stenosis. Proceedings of the 2nd World Congress on Medical Physics and Biomedical Engineering, 2000 (unpublished).
[72] Steinman, D. A., J. B. Thomas, H. M. Ladak, J. S. Milner, B. K. Rutt, and J. D. Spence. Reconstruction of carotid bifurcation hemodynamics and wall thickness using computational fluid dynamics and MRI. *Magn. Reson. Med*. 47:149–159, 2002.
[73] Tasciyan, T. A., R. Banerjee, Y. I. Cho, and R. Kim. Two-dimensional pulsatile hemodynamic analysis in the magnetic resonance angiography interpretation of a stenosed carotid arterial bifurcation. *Med. Phys.* 20:1059–1070, 1993.
[74] Taylor, C. A., M. T. Draney, J. P. Ku, D. Parker, B. N. Steele, K. Wang, and C. K. Zarins. Predictive medicine: Computational techniques in therapeutic decision making. *Comput. Aided Surg.* 4:231–247, 1999.
[75] Taylor, C. A., T. J. R. Hughes, and C. K. Zarins. Computational investigations in vascular disease. *Comput. Phys.* 10:224–232, 1996.
[76] Thomas, J. B., B. K. Rutt, H. M. Ladak, and D. A. Steinman. Effect of black blood MR image quality on vessel wall segmentation. *Magn. Reson. Med.* 46:299–304, 2001.
[77] Thompson, J. F., B. K. Soni, and N. P. Weatherill. Handbook of Grid Generation. Boca Raton, FL: CRC, 1998.
[78] Van Langenhove, G., J. J. Wentzel, R. Krams, C. J. Slager, J. N. Hamburger, and P. W. Serruys. Helical velocity patterns in a human coronary artery: A three-dimensional computational fluid dynamic reconstruction showing the relation with local wall thickness. *Circulation* 102:E22–E24, 2000.
[79] Vonesh, M. J., C. H. Cho, J. V. Pinto, B. J. Kane, D. S. Lee, S. I. Roth, K. B. Chandran, and D. D. McPherson. Regional vascular mechanical properties by 3D intravascular ultrasound with finite-element analysis. *Am. J. Physiol.* 272:H425–H437, 1997.
[80] Vorp, D. A., D. A. Steinman, and C. R. Ethier. Computational modeling of arterial biomechanics. *Comput. Sci. Eng.* 3:51–64, 2001.
[81] Wang, K. C., R. W. Dutton, and C. A. Taylor. Improving geometric model construction for blood flow modeling. *IEEE Eng. Med. Biol. Mag.* 18:33–39, 1999.
[82] Wentzel, J. J., J. Kloet, I. Andhyiswara, J. A. Oomen, J. C. Schuurbiers, B. de Smet, M. J. Post, D. de Kleijn, G. Pasterkamp, C. Borst, C. J. Slager, and R. Krams. Shear-stress

and wall-stress regulation of vascular remodeling after balloon angioplasty: Effect of matrix metalloproteinase inhibition. *Circulation* 104:91–96, 2001.

[83] Wentzel, J. J., R. Krams, J. C. Schuurbiers, J. A. Oomen, J. Kloet, W. J. Der Giessen, P. W. Serruys, and C. J. Slager. Relationship between neointimal thickness and shear stress after Wallstent implantation in human coronary arteries. *Circulation* 103:1740–1745, 2001.

[84] Yim, P. J., J. R. Cebral, R. Mullick, and P. L. Choyke. Vessel surface reconstruction with a tubular deformable model. *IEEE Trans. Med. Imaging* 20:1411–1421, 2001.

[85] Zhao, S. Z., X. Y. Xu, B. Ariff, Q. Long, A. V. Stanton, A. D. Hughes, and S. A. Thom. Interindividual variations in wall shear stress and mechanical stress distributions at the carotid artery bifurcation of healthy humans. *J. Biomech.* (in press).

[86] Zhao, S. Z., X. Y. Xu, M. W. Collins, A. V. Stanton, A. D. Hughes, and S. A. Thom. Flow in carotid bifurcations: Effect of the superior thyroid artery. *Med. Eng. Phys.* 21:207–214, 1999.

[87] Zhao, S. Z., X. Y. Xu, A. D. Hughes, S. A. Thom, A. V. Stanton, B. Ariff, and Q. Long. Blood flow and vessel mechanics in a physiologically realistic model of a human carotid arterial bifurcation. *J. Biomech.* 33:975–984, 2000.